SAND99-1306J

Magnetic Semiconductor Quantum Wells in High Fields to 60 Tesla: Photoluminescence Linewidth Annealing at Magnetization Steps

S. A. Crooker[1], D. G. Rickel[1], S. K. Lyo[2], N. Samarth[3] and D. D. Awschalom[4]

1) National High Magnetic Field Lab, MS E536, Los Alamos, NM 87545
2) Sandia National Lab, PO Box 5800 MS-1415, Albuquerque NM 87185
3) Department of Physics, Pennsylvania State University, University Park PA 16802
4) Department of Physics, University of California, Santa Barbara CA 93106

Abstract

Magnetic semiconductors offer a unique possibility for strongly tuning the intrinsic alloy disorder potential with applied magnetic field. We report the direct observation of a series of step-like reductions in the magnetic alloy disorder potential in single ZnSe/Zn(Cd,Mn)Se quantum wells between 0 and 60 Tesla. This disorder, measured through the linewidth of low temperature photoluminescence spectra, drops abruptly at ~19, 36, and 53 Tesla, in concert with observed magnetization steps. Conventional models of alloy disorder (developed for nonmagnetic semiconductors) reproduce the general shape of the data, but markedly underestimate the size of the linewidth reduction.

Sandia is a multiprogram laboratory operated by Sandia Corporation, a Lockheed Martin Company, for the United States Department of Energy under contract DE-AC04-94AL85000.

By their very nature, all semiconductor alloys possess some degree of compositional disorder. The magnitude and character of this intrinsic disorder are of keen interest to researchers and growers of alloyed semiconductors, who often rely on photoluminescence (PL) spectroscopy to infer material quality. Even in nominally "clean" alloys, the intrinsic compositional disorder leads to spatially varying exciton energies and inhomogeneously-broadened PL linewidths. Theoretical models [1,2] have been proposed to account for the observed PL linewidths in nonmagnetic alloys such as $Al_{1-x}Ga_xAs$ and $In_{1-x}Ga_xP$, where, for a given sample, the alloy fluctuation potential is fixed. However, a more rigorous test of these models would involve a material system in which the intrinsic disorder potential itself is tunable.

In contrast with nonmagnetic semiconductors, magnetic semiconductor alloys (*e.g.*, $Zn_{1-x-y}Cd_xMn_ySe$) offer the unique possibility for tuning the *magnetic* disorder potential in a single sample through the application of magnetic field. The local conduction and valence band edges near a magnetic Mn^{2+} cation are closely tied to its spin orientation through the strong J_{sp-d} exchange interaction between the band electrons and holes and the localized *d*-electrons that comprise the $S=5/2$ Mn^{2+} spin.[3] In a magnetic field, the local bandgap near a Mn^{2+} moment changes by $\frac{1}{2}(\alpha-\beta)\langle S_z\rangle$, where $\langle S_z\rangle$ is the expectation value of the Mn^{2+} spin and $(\alpha-\beta)$ is the J_{sp-d} exchange integral, usually of order 1 eV.[3,4] At low temperatures, even modest fields (H<1T) can dramatically shift – by hundreds of meV -- the effective bandgap near the Mn^{2+} cations, directly changing the alloy disorder potential seen by a microscopic probe (such as an exciton) and serving as a clear and direct test of present theoretical models.

In this paper, we show direct evidence for a field-induced annealing of the magnetic fluctuation potential in single ZnSe/Zn(Cd,Mn)Se magnetic quantum wells. A rapid reduction in the magnetic disorder, measured as a drop in PL linewidth, occurs at low fields (H<5T) as the isolated (paramagnetic) Mn^{2+} spins align, and then in stepwise fashion at high magnetic fields when antiferromagnetically-bound pairs of Mn^{2+} cations unlock. The magnitude of this stepwise linewidth annealing is over six times larger than predicted by present theories of disorder broadening in nonmagnetic semiconductor alloys, suggesting that revisions are required to include magnetic alloy disorder.

These high field PL measurements are enabled by the 60 Tesla Long-Pulse magnet at the National High Magnetic Field Laboratory (Los Alamos). Powered by a 1.4GVA motor-generator, the 2-second pulse duration of this magnet represents a hundred-fold increase in time "at field" as compared with traditional capacitor-driven pulsed magnets. Using high-speed CCD cameras [5], up to 2000 high-resolution (14-bit) optical spectra are acquired in a single 60 Tesla magnet shot, permitting timely reconstruction of the entire field dependence and clear resolution of small amplitude, wavelength, and linewidth shifts as a function of magnetic field. Light is coupled to and from the samples via single optical fibers, and temperatures down to 350mK are obtained with a fiberglass ^{3}He refrigerator. The field profile from the Long-Pulse magnet is shown in Figure 1a, where the field variation between spectra is at *most* ~165mT (inset, Fig.1a). The high light collection efficiency, low noise detector, and long pulse duration yields excellent signal-to-noise (>500) even with millisecond exposures and low laser excitation (<200μW at 400nm in all cases).

The samples are MBE-grown, 120Å wide ZnSe/$Zn_{.80}Cd_{.20}Se$ single quantum wells into which the magnetic species (Mn^{2+}, S=5/2) is "digitally" incorporated in the form of equally-spaced fractional-monolayer planes of MnSe.[6] We focus on samples containing 12 quarter-monolayer planes of MnSe (12x1/4ml) and 24 eighth-monolayer planes of MnSe (24x1/8ml). The wells are 39 monolayers wide, and since X-ray diffraction studies on "digital" superlattice samples reveal ~1 monolayer diffusion of Mn during growth, these structures have a nearly bulk-like 8% Mn concentration. To verify this, a 120 Å quantum well containing the quaternary magnetic alloy $Zn_{.70}Cd_{.22}Mn_{.08}Se$ was also grown, and was found to exhibit nearly identical PL properties (intensity and Zeeman shift), albeit with a slightly larger linewidth (8.5 meV vs. 6.8meV for the digital samples, at zero field). With applied field, the PL spectra become σ+ circularly polarized and show a large (~50meV) Zeeman redshift, corresponding to recombination of low energy electrons (s_z=-1/2) and holes (j_z=-3/2).[3] The dominant J_{sp-d} exchange interaction generates this large exciton spin splitting, and as such, the Zeeman shift of the PL peak reliably tracks (and is a measure of) the magnetization of the Mn^{2+} ensemble in the quantum well. [4]

Figure 1b shows the measured Zeeman shift ($\propto$ magnetization) from the 12x1/4ml quantum well to 60T. At low fields, the magnetization rises rapidly and saturates by ~8T. At higher fields, three magnetization steps are observed, corresponding to the partial unlocking of Mn-Mn nearest-neighbor pairs. As with all diluted magnetic semiconductors, the Mn^{2+} spins in these samples interact with one another predominantly via an antiferromagnetic J_{NN} exchange, which binds up neighboring Mn^{2+} moments in spin clusters of varying size.[7] Mn^{2+} singles, pairs, triples, and higher-order clusters occur with readily calculable probability assuming a well-defined (usually random) distribution of the Mn^{2+} moments.[8] Isolated Mn^{2+} moments (singles) behave as $S=5/2$ paramagnets with a Brillouin-like susceptibility. Nearest-neighbor pairs of Mn^{2+} spins bind to form a cluster with total spin $S_T=0$ at low fields. At low temperatures, when the applied field (H) is commensurate with the exchange energy ($H_n=2nJ_{NN}/g_{Mn}\mu_B$, $n=1,2,...,5$), the Mn-Mn pair "unlocks" and assumes total spin $S_T=1,2,...,5$, contributing a step in the magnetization. These magnetization steps are a well-studied signature of Mn-Mn pairs, from which can be determined the magnitude and nature of J_{NN}, as well as whether or not the Mn^{2+} spins are randomly distributed.[9] Larger spin clusters (triples, quadruples, etc) have increasingly complex susceptibilities which are usually modeled empirically.[10] The data in Fig. 1b is characteristic of all our samples – both the 24x1/8ml digital sample and the quaternary $Zn_{.70}Cd_{.22}Mn_{.08}Se$ quantum well elicit similar Zeeman shifts to within 5%, in support of the assertion that the distribution of Mn^{2+} in all the samples is nearly bulk-like. The magnetization steps at 18.8, 36.0, and 53.3 Tesla (+- 0.3T) are shown on an expanded scale in Fig. 2a. In practice, the fields H_n are not exact integer multiples due to distant-neighbor exchange fields between Mn moments which contribute a net offset. [11] However, the difference $H_{n+1} - H_n$ is expected to reflect the exchange energy, and we determine J_{NN}=-11.1K in these quaternary quantum wells.

Figure 2b shows the measured FWHM linewidth (Γ) of the PL spectra, obtained through a gaussian lineshape fit to the data. Γ(H) is characterized by a steady broadening, superimposed on which are a series of steplike reductions at low fields (H<5T), and at the Mn-Mn unlocking fields H_n. These data are interpreted as a series of field-driven reductions (*i.e.*, annealings) of the large local bandgap energy E_{MnSe} (=3.4eV) at magnetic Mn^{2+} sites. The slow (background) monotonic broadening of Γ is well understood from

previous work on nonmagnetic semiconductors and is due *only* to the field-induced shrinking of the exciton size. [1,2,12] We concentrate on the steplike reductions in Γ in the following. At low fields (H<8T), the ensemble of isolated $S=5/2$ Mn^{2+} spins in the quantum well evolves from a random orientation (with mean $\langle S_z \rangle = 0$ and variance $\left\langle (S_z - \langle S_z \rangle)^2 \right\rangle = 35/12$) to complete saturation ($\langle S_z \rangle = -5/2$, variance=0), reducing the local bandgap (and bandgap fluctuations) at Mn^{2+} sites and therefore reducing Γ (by 20-25%) in all magnetic samples. At the unlocking fields H_n, the Mn-Mn pairs ratchet into alignment with the applied field, lowering the local bandgap and thereby contributing an additional smoothing to the magnetic disorder potential seen by the exciton. The size of these stepwise annealings is most clearly shown in Figure 3, where the monotonic rise Γ due to the shrinking exciton has been subtracted off, and the data normalized. The stepwise disorder annealing is now plainly evident (a nonmagnetic control sample was also studied, and showed only the monotonic increase in Γ with field). To our knowledge, these data are the first to observe incremental annealings of the disorder potential in alloyed semiconductors.

As shown in Figure 3, the drops in Γ represent a 22%, 12%, 10%, and 4% relative decrease. These large changes in Γ are surprising since a random, 8% Mn^{2+} distribution would imply only ~3% of all cations sites are single Mn moments, and that less that 2% are Mn-Mn pairs. Indeed, existing models of disorder broadening do not account for the magnitude of the observed changes in Γ. In particular, the theories [1,2] of Schubert, Mena, Lee and Bajaj, and of Lyo (which share a common model for alloy disorder), *do* accurately describe the field- and concentration-dependent PL linewidths in nonmagnetic $Al_xGa_{1-x}As$ and $In_xGa_{1-x}P$, but do not reproduce the data from the magnetic alloys presented in this paper. While the general shape of the calculated Γ(H) is found to be quite reasonable, the magnitude of the observed linewidth steps are over six times larger than an adaptation of the above models predicts, as will be shown below. The following assumptions are common to all models of compositional disorder in alloyed semiconductors cited in Ref. 1: i) The constituents are randomly distributed; ii) Each cation site is assigned a local bandgap equal to the bandgap of its parent compound (*e.g.*, ZnSe or MnSe); and iii) Γ reflects the root-mean-square (rms) deviation of the average

bandgap within an exciton's wavefunction (or "volume"). We construct a similar model which also includes the field-dependent local bandgap of the Mn^{2+} cations which derives from the strong $J_{sp\text{-}d}$ exchange. We consider the samples to be $Zn_{.70}Cd_{.22}Mn_{.08}Se$ alloys, comprised of cations of Zn, Cd, isolated Mn^{2+} spins, paired Mn^{2+} spins, and Mn^{2+} spins locked in larger clusters (triples, quadruples, etc). These cations occur with concentration P_1, P_2, P_3, P_4, and P_5 respectively, and have local bandgaps $\Delta_1 = E_{ZnSe}$ = 2.82 eV, $\Delta_2 = E_{CdSe}$ = 1.87 eV, and $\Delta_3 = \Delta_4 = \Delta_5 = E_{MnSe} + \frac{1}{2}(\alpha - \beta)\langle S_z \rangle$. Here, E_{MnSe} = 3.4eV, $\langle S_z \rangle$ is the expectation value of the Mn^{2+} spin, and the exchange integral $(\alpha - \beta)$ = 1.37eV is the magnitude of the $J_{sp\text{-}d}$ exchange interaction between the Mn^{2+} cation and the conduction and valence bands, chosen to be that from $Zn_{1-x}Mn_xSe$.[3] The probabilities of single, paired, and higher order Mn^{2+} clusters (P_3, P_4, and P_5) equal 3.0%, 1.7%, and 3.3% respectively (assuming a random 8% Mn^{2+} distribution).

Following standard treatments of DMS systems[3,4], isolated Mn^{2+} spins obey a modified Brillouin function, $\langle S_z \rangle = -\frac{5}{2} B_{5/2}\left(5\mu_B g_{Mn} H / 2k_B T^*\right)$, where T^*=3.5K is an empirical "effective temperature" which best fits the low-field susceptibility. For the Mn^{2+} spins in pairs, $\langle S_z \rangle = -\frac{1}{2} S_T$, where $S_T = \sum \left[1 + \exp\left(g_{Mn}\mu_B(H_n - H)/k_B T\right)\right]^{-1}$ = 0,1,...,5 is the total spin of the pair. For spins in higher-order clusters, we consider $\langle S_z \rangle$ = -½ at high fields (>8T), a reasonable approximation for triples and in accord with standard treatments for larger clusters.[7] As our interest is in calculating the *relative* (rather than absolute) changes Γ which occur when Mn^{2+} spins align, we do not attempt a detailed description of the size and shape of the exciton wavefunction, which ultimately enters into Γ as a prefactor. The heart of the model – calculation of the rms fluctuation of the energy gap – remains identical to previous models [1].

Given an exciton energy $E = N^{-1}\sum E_j$ (j=1,...,N; the mean bandgap of the N lattice sites within the exciton wavefunction), and an ensemble average $\mu = \langle E \rangle = \sum P_i \Delta_i$ (equal to PL line-center), we compute the variance

$$\sigma^2 = \left\langle (E - \mu)^2 \right\rangle = N^{-1}\left(\sum P_i \Delta_i^2 - \mu^2\right), \qquad (1)$$

where $\Gamma = 2\sqrt{2\ln 2}\sigma$. As written, however, equation (1) does not implicitly account for the Boltzmann distribution of the isolated Mn^{2+} spins, which present an additional fluctuation that must be calculated separately, namely

$$P_3\Delta_3^2 \equiv P_3 \sum Z^{-1} e^{-g_{Mn}\mu_B H S_z / k_B T} \left(E_{MnSe} + \tfrac{1}{2}(\alpha - \beta)S_z\right)^2, \quad (2)$$

where Z is the Mn^{2+} partition function and the sum is over the spin multiplet $S_z = -\tfrac{5}{2}, -\tfrac{3}{2}, \ldots, +\tfrac{5}{2}$. This additional fluctuation affects only the initial drop in Γ (H<8T), before the isolated Mn^{2+} spins saturate. The individual spins within Mn-Mn pairs are not treated similarly, due to their correlated nature – unlike isolated spins, fluctuations of the individual Mn^{2+} spins within a pair do *not* affect the exciton energy E, because the total spin S_T is fixed. Equations (1) and (2) yield Γ=8.22meV (assuming a spherical exciton wavefunction of radius 60Å).

The dotted line in Fig. 3 shows the calculated Γ(H), where it is clear that the model considerably underestimates the magnitude of the observed changes in Γ. The calculated initial drop in Γ (from the isolated Mn^{2+} spins) is only half as large as observed, and the drop at H_1 and H_2 (shown expanded in Fig. 4) is of order 2% and 1%, more than six times smaller than observed. On the other hand, the model does admirably reproduce the general shape of the data (Fig. 4), showing the comparatively large initial decrease, stepwise drops at H_n which decrease in size, and even the shallow local minimum observed at ~4T in the digital samples. The model is quite robust against reasonable (~10%) uncertainty in the bandgaps Δ_i, the concentrations P_i, and the exchange integral $(\alpha-\beta)$; for comparison, Fig. 4 also shows the calculated results assuming a 25% larger Mn concentration (dotted line), and a 20% decrease in $(\alpha-\beta)$ (dashed line), with little change. Even with grossly inaccurate input parameters, such as the assumption of *all* isolated, or *all* paired Mn spins, the model underestimates the size of the initial drop in Γ, or the relative drop at magnetization steps (not shown). Of interest, the model predicts stepwise *increases* in Γ at the 4th and 5th steps, at ~71T and ~88T (inset). Midway through the 3rd magnetization step (for $(\alpha-\beta)$=1.37eV), the local bandgap of the Mn-Mn pairs drops *below* the mean bandgap (μ), thus increasing the fluctuation potential once again. We anticipate that experiments in higher magnetic fields (or in samples with smaller J_{NN}, *e.g.* CdMnTe) will exhibit this behavior.

While the qualitative field dependence of Γ is well reproduced by our model, the magnitude of the stepwise reductions remains puzzling, suggesting that at least one of the underlying assumptions of the model is in error. For example, the assignment of a local, $J_{sp\text{-}d}$ exchange-driven bandgap to each Mn^{2+} cation site may be insufficient -- while this approach works well as a starting point for mean-field treatments of general magneto-optical properties in dilute magnetic semiconductors[3,4], it may be inadequate for the computation of disorder. More likely, the large alloy fluctuations presented by the Mn^{2+} may act as electron and hole pinning centers, thus causing significant de-localization of the excitons when the magnetic alloy disorder is annealed at low fields and at the magnetization steps. De-localization of the exciton wavefunction leads directly to an additional reduction in Γ (see Eqn. 1). For example, a 23%, 20%, and 8% relative increase in exciton "volume" at H_1, H_2, and H_3 would lead to an additional 10%, 9%, and 4% relative drop in Γ, thereby reproducing the data very well. However, an accurate calculation of exciton de-localization based on a reduction in alloy disorder must await a more detailed theoretical treatment.

In summary, the long duration of the 60T Long-Pulse magnet permits direct observation of an incremental annealing of the magnetic disorder potential at magnetization steps in ZnSe/Zn(Cd,Mn)Se single quantum wells through the linewidth of PL spectra. While Mn-Mn pairs comprise less than 2% of all cations, the relative decrease in Γ at the magnetization steps is as large as 12%. A model of the magnetic alloy disorder, based on models for nonmagnetic III-V systems, reproduces the general shape of the data but underestimates the size of the steps in Γ, suggesting that a new theory is required to properly account for magnetic disorder in alloyed semiconductors.
We gratefully acknowledge the technical assistance of M. Pacheco and W. Bowman, and support from grants NSF DMR 97-01072 and 97-01484 and U.S. DOE Contract #DE-AC04-94AL85000.

References

[1] E. F. Schubert *et al.*, Phys. Rev. B **30**, 813 (1984); R. A. Mena *et al.*, J. Appl. Phys. **70**, 1866 (1991); S. M. Lee and K. K. Bajaj, J. Appl. Phys. **73** 1788, (1993).

[2] S. K. Lyo, Phys. Rev. B, **48**, 2152 (1993).

[3] J. K. Furdyna, J. Appl. Phys. **64**, R29 (1988).

[4] R. L. Aggarwal *et al.*, Phys. Rev. B, **32**, 5132 (1985).

[5] Princeton Instruments LN/CCD-1340/100-EB.

[6] S. A. Crooker *et al.*, Phys. Rev. Lett. **75**, 505 (1995).

[7] Y. Shapira, J. Appl. Phys. **67**, 5090 (1990); Y. Shapira *et. al.*, Phys. Rev. B, **33**, 356 (1986).

[8] Y. Shapira *et al.*, Phys. Rev. B, **30** 4021 (1984); R. E. Behringer, J. Chem. Phys. **29**, 537 (1958).

[9] V. Bindilatti *et al.*, Phys. Rev. Lett., **80**, 5425 (1998); S. Foner *et al.* , Phys. Rev. B, **39**, 11793, (1989).

[10] D. Heiman, E. D. Isaacs, P. Becla, and S. Foner, Phys. Rev. B, **35**, 3307 (1987).

[11] B. E Larson, K. C. Hass, R. L. Aggarwal, Phys. Rev. B, **33**, 1789 (1986).

[12] E. D. Jones, R. P. Schneider, S. M. Lee, K. K. Bajaj, Phys. Rev. B, **46** 7225 (1922).

Figure Captions

Fig. 1 a) The field profile of the 60 Tesla Long-Pulse magnet (and a capacitor-driven magnet for comparison). Inset: Expanded view; optical spectra are acquired at each point. b) The Zeeman shift ($\propto$ magnetization) of the PL peak from the 12x1/4ml MnSe quantum well, showing a Brillouin-like saturation followed by steps.

Fig. 2 a) Magnetization steps in the 12x1/4ml sample. b) PL linewidth (Γ) from the12x1/4ml, 24x1/8ml, and quaternary ZnCdMnSe quantum wells (bottom to top). Drops in Γ correlate with the magnetization steps. The steady, superimposed broadening arises from the shrinking exciton.

Fig. 3 The normalized linewidth (the broadening due to the shrinking exciton has been subtracted). At the magnetization steps, relative drops of 12%, 10%, and 4% are observed. The dotted line is the calculated $\Gamma(H)$ based on existing theories.

Fig. 4 a) The calculated $\Gamma(H)$, based on existing models of alloy disorder (solid line). Dashed (dotted) line shows calculated results for different values of the $J_{sp\text{-}d}$ exchange (Mn concentration). Inset: The model to 100 Tesla, predicting steplike *increases* in Γ at higher fields.

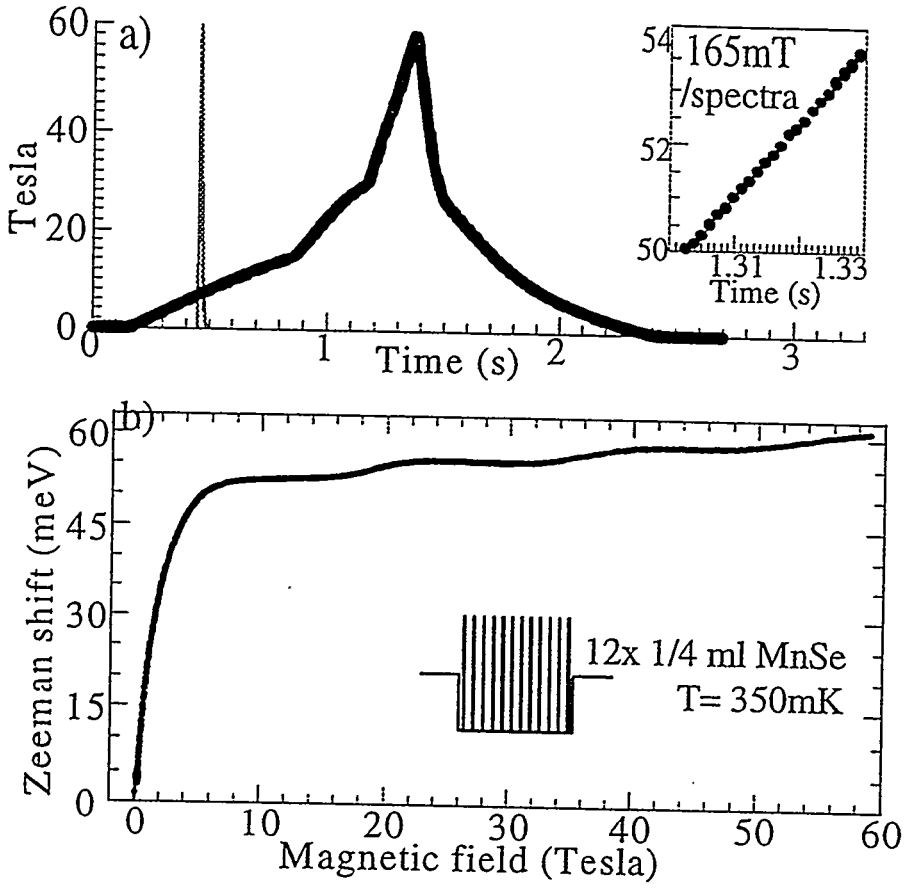
a)
Tesla
60
40
20
0
0
1
Time (s)
2
3
54
165mT
/spectra
52
50
1.31
1.33
Time (s)
b)
Zeeman shift (meV)
60
45
30
15
0
12x 1/4 ml MnSe
T= 350mK
0
10
20
30
40
50
60
Magnetic field (Tesla)

Fig. 1

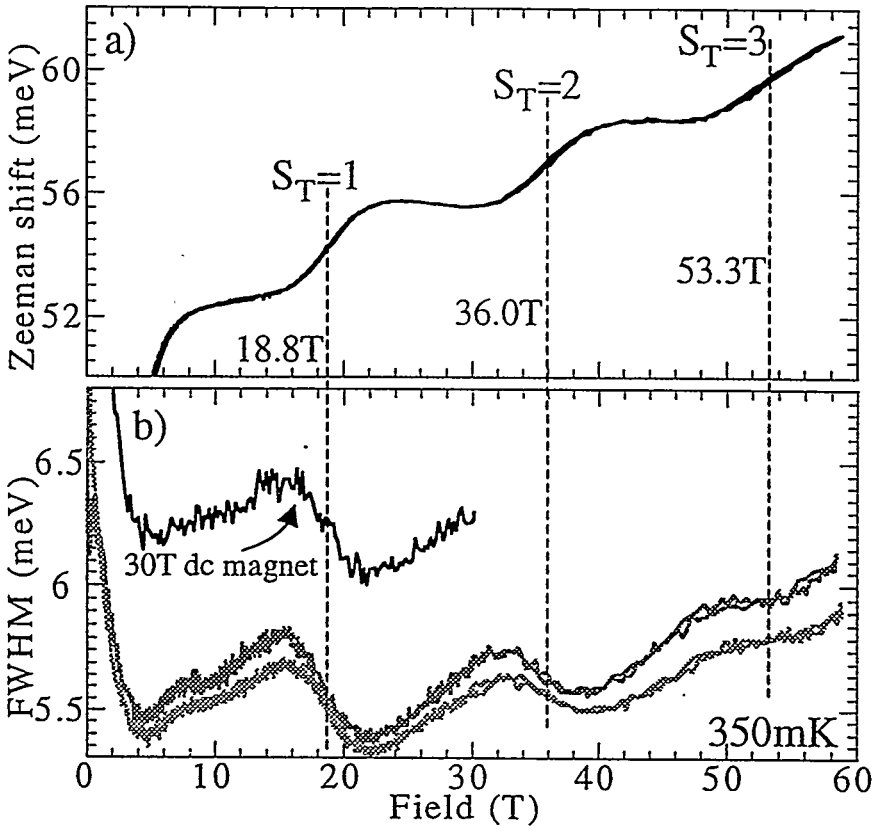
a)
b)
Zeeman shift (meV)
FWHM (meV)
Field (T)
S_T=1
S_T=2
S_T=3
18.8T
36.0T
53.3T
30T dc magnet
350mK
60
56
52
6.5
6
5.5
0
10
20
30
40
50
60

Fig. 2

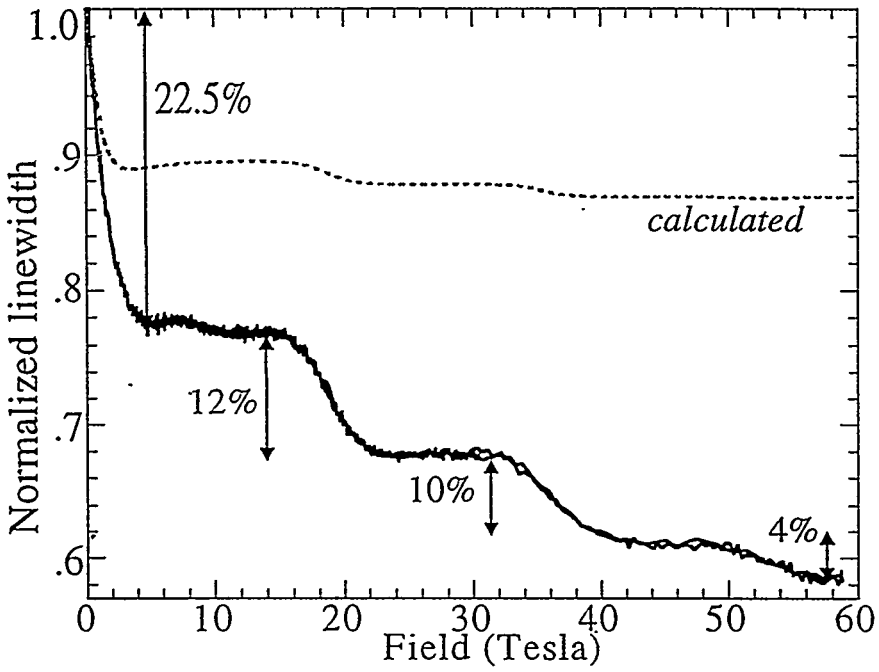
1.0
.9
.8
.7
.6
Normalized linewidth
22.5%
calculated
12%
10%
4%
0
10
20
30
40
50
60
Field (Tesla)

Fig. 3

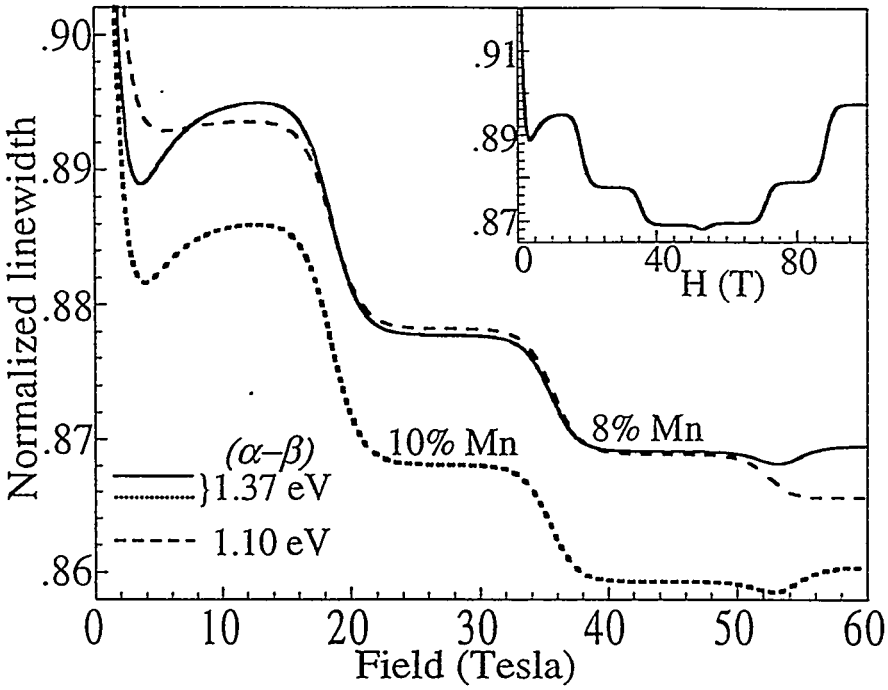
.90
.89
.88
.87
.86
Normalized linewidth
0
10
20
30
40
50
60
Field (Tesla)
(α–β)
1.37 eV
1.10 eV
10% Mn
8% Mn
.91
.89
.87
0
40
80
H (T)

Fig. 4